Construction and Building Materials 99 (2015) 82–89

Contents lists available at ScienceDirect

Construction and Building Materials

journal homepage: www.elsevier.com/locate/conbuildmat

Mechanical performance of ECC with high-volume fly ash after sub-elevated temperatures

Jiangtao Yu [a], Jianhui Lin [a], Zhigang Zhang [b], Victor C. Li [b,*]

[a] College of Civil Engineering, Tongji University, Shanghai 200092, China
[b] School of Transportation, Southeast University, Nanjing 210096, China

HIGHLIGHTS

- A proper temperature treatment effectively improves the tensile performance of ECC with high-volume fly ash.
- ECC controls the crack width effectively after temperature treatment of no more than 200 °C.
- The improvement of interface properties enhances strain capacity of ECC with high-volume fly ash.
- This study provides a possible technique to improve ECC's mechanical properties.

ARTICLE INFO

Article history:
Received 20 June 2015
Received in revised form 1 September 2015
Accepted 3 September 2015

Keywords:
Engineered cementitious composites
Fly ash
Elevated temperature
Tensile property
Interface property

ABSTRACT

Engineered cementitious composites (ECC) are known for their strain-hardening behavior under tension, and have been increasingly applied in engineering practice. However, the lack of understanding about the performance of ECC exposed to elevated temperatures limits their application in some special fields. Therefore, the residual mechanical performance of ECC containing very high volume fly ash (FA/C = 4.4) and polyvinyl alcohol fibers (HVFA-ECC) was investigated after temperature exposures of 20 °C, 50 °C, 100 °C and 200 °C, considering the melting temperature of polyvinyl alcohol fiber is about 230 °C. The test results indicated that HVFA-ECC maintains its unique multiple cracking and pseudo strain hardening characteristics after temperature exposure within this range. The tensile properties, including the ultimate tensile strength and tensile strain capacity, increased after the 50 °C and 100 °C treatments, but diminished after the 200 °C exposure. To better understand the impacts of thermal exposure, tests were carried out on the fiber tensile strength, fiber/matrix interfacial bond and matrix fracture toughness. It was found that the fiber's tensile strength retained its room temperature value up to 100 °C exposure, but dropped significantly after undergoing the 200 °C heating. The interface parameters (chemical bonding G_d and frictional bonding τ_0) and the strain-hardening index (J_b'/J_{tip}) have a similar trend as the composite tensile properties, which explained the variation of composite response with thermal treatment. The test results indicates that HVFA-ECC can resist a sub-elevated temperature ($\leqslant$200 °C) exposure, and a moderate temperature treatment ($\leqslant$100 °C) may actually enhance ECC's tensile properties. This study provides a scientific basis for further development of ECC for elevated temperature applications and also a possible technique to improve ECC's mechanical properties.

1. Introduction

At present, high-performance concrete, according to their superior mechanical property, can be roughly classified into two categories: high-compressive-strength concretes [1,2] and high-tensile-ductility concretes (for example, engineered cementitious composite [ECC], strain-hardening cement composites [SHCC], and some high-performance fiber-reinforced cementitious composites [HPFRCCs]) [3,4]. Both types of concrete have their advantages in engineering applications. High-strength concrete can effectively reduce the size of structural members and provide additional strength safety margins (particularly in compression) for reinforced concrete structures. Generally, high ductility concrete can maintain a portion of its tensile capacity under

* Corresponding author at: Department of Civil and Environmental Engineering, University of Michigan, Ann Arbor, MI 48109-2125, USA.
E-mail address: vcli@umich.edu (V.C. Li).

http://dx.doi.org/10.1016/j.conbuildmat.2015.09.002
0950-0618/

considerable deformation and enhance the structure's reliability during extreme loading events, such as earthquakes, hurricanes or blasts.

Engineered cementitious composites (ECC) is a special class of high-tensile-ductility concretes. Unlike the typical trial-and-error material development methodology, ECC is designed based on micromechanics theory, resulting in a tensile strain capacity of more than 3%, while keeping the fiber volume fraction no greater than 2% [5,6]. The ductility of ECC is on the order of several hundred times that of normal concrete or fiber reinforced concrete (FRC). ECC exhibits multiple cracking during strain-hardening with micro-crack width less than 100 μm [7], making it a highly durable material in a wide variety of environmental exposure conditions, including chloride [8], high alkalinity [9], and freeze–thaw exposures [10].

Due to its high tensile ductility and durability, ECC is attractive in a variety of civil engineering application. As example, it has been applied to pavement, structural slabs, high-rise buildings and has also been used in structural repair and retrofits [11,12]. During the service life, fire is one of the most serious risks to all structures. It is widely reported e.g. [13,14] that high temperatures (>200 °C) will cause physical and chemical changes in normal cement based materials, resulting in deteriorations in mechanical properties, such as compressive strength and modulus of elasticity. Most ECCs are reinforced with polymeric fibers with relatively low melting temperature so that even sub-elevated temperature below 200 °C may be a concern. With the broadening application of ECC, it becomes increasingly important to understand the mechanical performance of ECC at sub-elevated temperatures. Applications where the tensile ductility of ECC is useful, and which the material may be exposed to a moderately elevated temperature, includes certain energy infrastructure such as nuclear power plants, casings in oil field, certain airfield pavements, and building and transportation infrastructures with limited fire exposure.

In recent years, a limited number of studies have focused on the performance of polyvinyl alcohol fiber ECC (PVA-ECC) subjected to temperature exposures. Sahmaran, et al. [13,15] tested the post-fire properties of PVA-ECC with two different contents of fly ash as a replacement for cement (55 and 70% by weight of total cementitious materials). After 200 °C, 400 °C, 600 °C and 800 °C heating treatment for one hour, the residual mechanical properties (compressive strength, compressive stress–strain curve and stiffness) and mass loss were examined. Results indicated that the fire resistance of the cementitious matrix was substantially improved with PVA fiber, and the risk of explosive spalling often observed in normal concrete was eliminated. Yu et al. [14] studied the influence of cooling regimes on the compressive strength of PVA-ECC that had been exposed to elevated temperatures. Water quenching at 800 °C was found to improve the strength recovery of ECC. The tensile capacity of ECC after elevated temperature was not reported in the aforementioned studies.

Bhat et al. [16] observed that the tensile strain capacity decreased with temperature exposure (2 h) up to 200 °C, but maintained the strain-hardening feature of ECC (FA/C = 1.9). At higher temperatures, the PVA-ECC loses its ductility all together. A similar finding of diminished strain capacity was obtained by Mechtcherine et al. [17] for ECC (FA/C = 1.2) specimens exposed to various temperatures up to 150 °C for one hour. These studies indicate that ECC, if properly designed, may retain its useful tensile ductility at moderately elevated temperature below the melting point of the reinforcing fiber.

In this study, the focus is on the tensile stress–strain response and crack pattern development of a high fly-ash content (FA/C = 4.4) PVA-ECC exposed up to 200 °C. Experiments were conducted on composite macro scale, including tensile tests and compressive test after sub-elevated temperature exposures. A digital image correlation analysis was used to investigate the tensile crack pattern development. Fundamental understanding of the composite behavior under sub-elevated temperature is provided by meso-scale studies, including tensile test on single fiber, single fiber pull out test, single crack tensile test and matrix fracture toughness test, carried out on the PVA-ECC ingredients also subjected to the same temperature exposure range. The results from tests on meso-scale revealed the temperature impacts on the tensile strength of fiber, the residual chemical bonding (G_d), frictional bond (τ_o), and on the strain-hardening index J'_b/J_{tip} (J'_b is the fiber bridging complementary energy and J_{tip} matrix toughness). The test results on the meso-scale provide insights on the change of mechanical performance of HVFA-ECC after sub-elevated temperature exposure.

2. Experimental investigations on the composite macro-scale

The experimental study contains two parts: The first part examines the influence of sub-elevated temperatures on the macro-mechanical performance of ECC, particularly tensile properties. The second part analyzes the mechanisms of thermal impacts at the mesoscopic scale, including changes in fiber strength, fiber/matrix interfacial bond and matrix fracture toughness.

2.1. Material and specimen preparation

Table 1 lists the adopted mixture proportion to produce ECC material. ASTM Type I Portland cement and Class F fly ash were used. The silica sand used has maximum and average grain size of 250 μm and 110 μm, respectively. The PVA fiber, with a surface oil coating of 1.2% by weight was used at 2% volume content. The mechanical and geometrical properties, and melting point, of the PVA fiber are summarized in Table 2.

All mixtures were prepared in a Hobart type mixer of 15 L capacity. All solid dry raw materials include cement, sand and fly ash were mixed for 1 min. Water and water reducer (ADVA-190) were added and mixed for another 3 min until the paste reached good fluidity. Finally, the fiber was added slowly into the mortar and mixed for 5 min until the fibers were well dispersed. The fresh ECC was cast into the molds and covered with plastic sheets, and subsequently demolded after 1 day curing. All specimens were cured for another 27 days in air before testing.

The test matrix is shown in Table 3, listing the number of specimens for each test case. Except for the control group (20 °C), all specimens were heated in an electric furnace to the target temperatures of 50 °C, 100 °C or 200 °C at a heating rate of 10 °C/min and maintained for 1 h to ensure a steady-state thermal condition. After these temperature exposures, the specimens were cooled naturally in air.

No cracking or flaking can be observed on the surface of dogbone specimens after heating (Fig. 1). No significant color change in matrix or fiber was observed in the cases of 50 °C or 100 °C. After 200 °C heating, the dogbone surface appeared slightly yellow, while the color of fibers turned into brown, indicating a chemical change in PVA fibers, as shown in Fig. 1.

All specimens were wrapped in plastic until loading tests. Cube specimens with dimension of 50.8 × 50.8 × 50.8 mm were tested on a FORNEY F50 machine (±10 N resolution) with a load control scheme to obtain the maximum compressive strength.

Dogbone-shaped specimens (Fig. 2), recommended by the Japan Society of Civil Engineers (JSCE) [18], were adopted for standardized testing of ECC. Two external linear variable differential transformers (LVDTs) with a range up to 100 mm were fixed on the surface of the dogbone specimens to measure the displacement. Digital image correlation (DIC) [19] method was applied to monitor the tensile crack pattern development of the dogbone specimens. During testing, A CCD camera took pictures of the speckle pattern and made grey scale images. DIC visualizes 2D displacement fields, and as a consequence strain fields, by comparing subsequent pictures taken of a speckle pattern on the surfaces of the dogbone. Apart from displacement and strain fields, cracks can also be characterized as discontinuities in the displacement field, making DIC a powerful tool to analyze the crack's initiation and propagation. Moreover, by acquiring the displacement values between two adjacent cracks and eliminating the deformation from non-cracked matrix by strain integrating, the crack width can be easily obtained. With the acquired data, the crack width and number were automatically calculated using Matlab.

Table 1
Mixture proportion of ECC (kg/m^3).

Cement	Fly ash	Water	PVA fiber	Sand	ADVA-190	W/(C + FA)	FA/C
232	1019	325	26	450	4.3	0.26	4.4

Table 2
Properties of PVA fiber.

Diameter, μm	Length, mm	Nominal strength, MPa	Modulus, GPa	Density, kg/m^3	Melting point, °C
39	12	1600	42	1300	230

A batch of single PVA fibers with the uniform length of 100 mm were tested to obtain the temperature effect on fiber's tensile strength. A batch of single PVA fibers were embedded inside cementitious matrix with 0.7–1.5 mm embedment length for the following fiber pull-out test. The detailed specimen preparation procedure can be found in literature [20]. The general profile of a single fiber pull-out curve can be decomposed into three major regimes: debonding, pull-out and fiber rupture process (Fig. 3) [20]. Initially, a stable fiber debond process occurs along the fiber/-matrix interface. The load resisted by fiber bonding to matrix increases up to P_a as the debonded length, l_d, increases towards l_e. Then sudden load drop from P_a to P_b is associated with the complete loss of chemical bond, and whole fiber slippage begins. The chemical debonding energy value (G_d) is calculated from the P_a to P_b difference accordingly to Eq. (1). From P_b value, the frictional bond strength τ_o at the onset of fiber slippage can be computed according to Eq. (2). After debond process, the load increases further due to the slip-hardening during the fiber sliding process.

$$G_d = \frac{2(P_a - P_b)^2}{\pi^2 E_f d_f^3} \quad (1)$$

$$\tau_o = \frac{P_b}{\pi d_f l_e} \quad (2)$$

where E_f = fiber Young's modulus, and d_f = fiber diameter.

To figure out the influence of temperatures on matrix's toughness, matrix toughness testing was conducted in accordance with ASTM E399 [21]. Notched prism specimens with dimensions of 305 × 76 × 38 mm were prepared according to the mixture proportion (without PVA fiber) listed in Table 1. A single notch with width of 1.5 mm was cut using a diamond saw before testing at the mid-span to a depth of 40% of prism depth. Notched specimens were carried out on a MTS servo hydraulic test machine in the fire resistance laboratory at Tongji University (Fig. 4). Three specimens were tested for each test series.

To obtain the composite tensile stress crack-opening relationship of ECC, a dogbone specimen containing a circumferential notch with width of 1 mm and with a residual sectional dimensions about 20 × 8 mm was used. Fig. 5 shows the test setup.

All tensile tests were conducted on an Instron pneumatic servo electronic tensile machine in the ACE-MRL at University of Michigan (±0.1 N resolution). A uniform displacement control scheme with the rate of 0.2 mm/min was engaged, except for the single fiber pull-out test, of which the load rate was 0.1 mm/min.

2.2. Effect of temperature exposure on the composite residual compressive strength

The influence of elevated temperatures on the compressive strength of ECC cubes is shown in Fig. 6. Each data point is an average from at least three compression tests. As shown in Fig. 6, there is no obvious change for compressive strength after the 50 °C and 100 °C exposures. The compressive strength increased by 3.9% at 50 °C and by 1.3% at 100 °C, but dropped 20% at 200 °C, as compared with the control specimens tested at ambient temperature. This suggests degradation of the cementitious matrix at 200 °C, as also observed by Blat et al. [16].

2.3. Effect of temperature exposure on the composite residual tensile properties

Uniaxial tensile test is considered the most convincing way to validate the strain-hardening characteristic of ECC. Fig. 7 plots the tensile stress–strain curves of dogbone specimens after subjected to different temperatures. All curves demonstrate the typical characteristic of ECC: the initial elastic stage, the strain-hardening stage and the tension-softening stage. Table 4 lists the residual tensile properties. As shown, all the average ultimate tensile strain exceeded 2%. Fig. 8 presents the ultimate strength and tensile strain capacity of all specimens. Specimens at 20 °C exhibit a tensile strain capacity of 2.68% and ultimate strength of 3.83 MPa on average. After 50 °C and 100 °C exposure, the ultimate tensile strength increases to 4.07 MPa and 4.91 MPa, while the tensile strain capacity enhances to 3.66% and 4.68%. However, after undergoing 200 °C heating, the tensile strength and strain capacity decreases to 3.97 MPa and 3.10% respectively, close to the room temperature values.

Table 3
Experimental test matrix (specimen number).

Temperature, °C	20	50	100	200
Compressive strength test	3	3	3	3
Dogbone tensile test	6	6	6	6
Fiber strength test	4	4	3	5
Single fiber pull-out test	4	3	3	3
Three-point bending test	3	3	3	3
Single crack tensile test	3	3	3	3

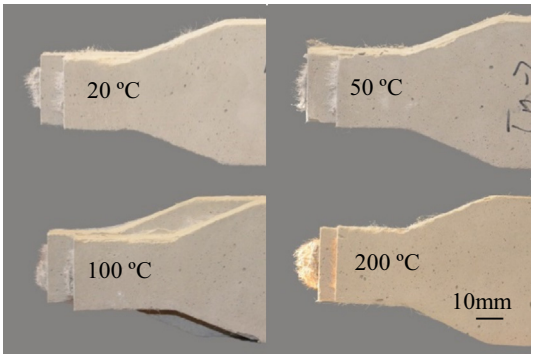

Fig. 1. Specimen surface appearance after temperature exposures.

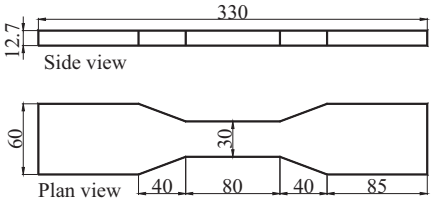

Fig. 2. Dogbone specimen for ECC tensile test (Note: All dimensions in mm.).

The turning point in the tensile stress–strain curve (Fig. 7) indicates the first crack of matrix under tension. Normally, the determination of this turning point involves some subjectivity. In this paper, the Digital Image Correlation (DIC) method is applied to all the dogbone specimens in tensile test to objectively obtain the cracking strength of HVFA-ECC through analyzing the DIC strain contour. Fig. 9 shows an example. The appearance of the first crack can be observed clearly in Fig. 9. The position of the lines on the top or bottom side of the DIC picture denotes the crack distribution on the surface of dogbone specimen, and the line height is made proportional to the crack width.

The influence of temperature on the first cracking strength is shown in Fig. 10. Initial increase of temperature enhances the first cracking strength. At 100 °C, the cracking strength attains the peak value, which is 129% that of 20 °C. However, the cracking strength of the specimens exposed to 200 °C is reduced to 2.67 MPa, nearly equal to the cracking strength of the control specimens.

2.4. Effect of temperature exposure on composite residual crack pattern

A similar trend was also observed in the crack pattern. The crack width and the number of cracks were calculated based on the post-processing results from DIC (Fig. 9). Fig. 11 reveals the relationship between crack number and tensile stress development in ECC. It demonstrates the typical characteristic of ECC materials. After first crack at the end of initial elastic stage, multiple cracks develop as stress increases within a narrow range.

Three specimens were tested at each temperature. Fig. 12 presents the crack number and crack width at peak load for each temperature exposure case. It is found that temperature exposure has little impact on crack width, but has a strong influence on the crack number. The crack number in ECC specimen rises as the exposure temperature increases from 20 °C to 100 °C, ranging from 32 to 51, but decreases to 36 for the temperature exposure of 200 °C, very close to crack number of 32 at 20 °C. It indicates that an appropriate temperature treatment up to about 100 °C can trigger more cracks and enhance the tensile strain capacity of ECC with high fly ash content.

3. Discussion and experimental investigation on the composite meso-scale

To further explore the temperature treatment's impacts, fiber tensile strength test, single fiber pull-out test, single crack tensile test and matrix fracture toughness test were carried out. As a result, fiber strength, fiber/matrix interface properties and matrix

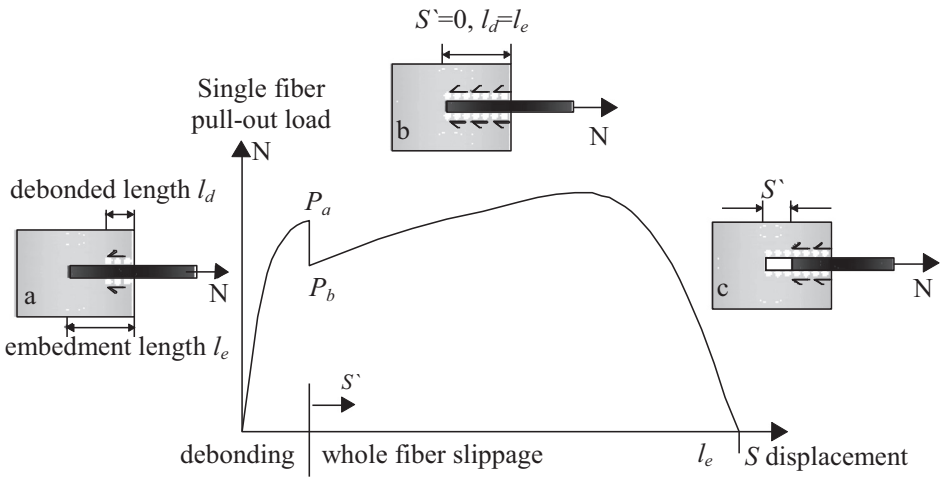

Fig. 3. The stages of fiber pullout, for interpretation of fiber/matrix interface properties.

Fig. 4. Three-point bending test.

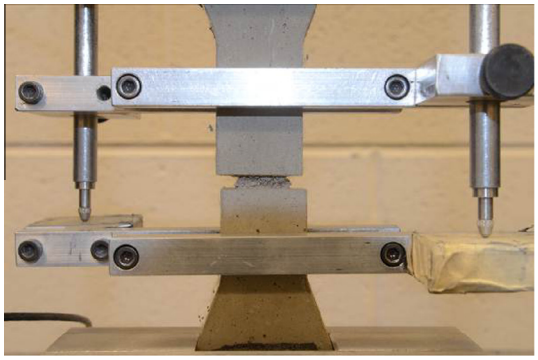

Fig. 5. Single crack tensile test.

fracture toughness at sub-elevated temperatures were obtained to shed light on the influence of heat treatment on the mechanical behavior of HVFA-ECC.

3.1. Effect of temperature on residual tensile strength of fiber

The tensile strength of PVA fiber may be one factor affecting the mechanical properties of ECC after undergoing sub-elevated temperatures. The residual fiber strengths are summarized in Fig. 13. The results indicate fibers exposed to 50 °C and 100 °C remain essentially unchanged from its room temperature (20 °C) value.

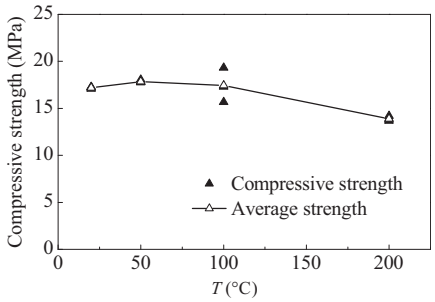

Fig. 6. The effects of temperature exposures on 28 day compressive strength.

However, the average tensile strength of fiber drops to 800 MPa after exposure to 200 °C. The decrease of fiber strength at 200 °C may be one reason behind the reduction in ultimate tensile strength and strain capacity of ECC exposed to 200 °C treatment, compared with those of specimens exposed to 100 °C treatment.

3.2. Effect of temperature on the residual interface properties

Single fiber pull-out test was adopted to determine the fiber/-matrix interface properties [6,22,23] after subjected specimens to sub-elevated temperatures. The residual chemical bonding (G_d) and frictional bond (τ_o) after temperature exposures were determined from the pull-out test data. The influences of temperature treatment on G_d and τ_o are shown in Fig. 14. G_d increases as treatment temperature rises from 20 °C to 50 °C to 100 °C, then drops drastically at 200 °C. τ_o increases with treatment temperature at 50 °C and decreases slightly at 100 °C, then drops distinctly at 200 °C. Pulling out 39 μm diameter PVA fibers with about 1 mm embedded lengths out of cementitious matrix, considerable scatterings were observed in G_d and τ_o. The similar reports were found in literature [20,22,23].

The initial increase in G_d and τ_o with temperature treatments may be explained as follows: As a large amount of fly ash and a low ratio of water/binder are used in the HVFA-ECC, the continued hydration of cement and pozzolanic reaction of fly ash after 28 days are accelerated by exposure to higher temperature. The build-up of hydration products in the interfacial transition zone (ITZ), in particular calcium hydroxide, should increase the fiber/-matrix chemical bond [24]. In addition, moisture loss in ECC caused by temperature exposure, as observed by Bhat et al. [16], implies release of free water in large pores and small capillary pores. The

Table 4
Tensile properties of ECC.

Temperature, °C	Ultimate tensile strength, MPa	Tensile strain capacity, %	Cracking strength, MPa
20	3.83 ± 0.71	2.68 ± 1.18	2.63 ± 0.62
50	4.07 ± 0.63	3.66 ± 0.74	2.88 ± 0.37
100	4.91 ± 0.85	4.68 ± 0.42	3.39 ± 0.39
200	3.97 ± 0.23	3.10 ± 0.44	2.67 ± 0.47

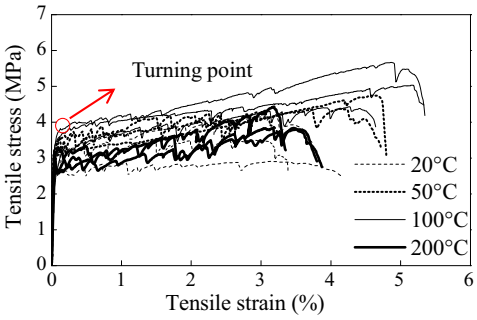

Fig. 7. The effects of temperature exposures on tensile stress–strain curves.

evaporation of free water leads to greater Van der Waal's force. As a result, the cement gel layers move closer to each other [25,26], thus increasing the compactness of ITZ and consequently, the interface frictional bond. On the other hand, when the temperature rises further (e.g. at 200 °C), the free water vaporizes completely from the matrix and internal vapor pressure promotes micro-cracking damage in matrix as well as degradation of interface properties.

3.3. Effect of temperature exposure on matrix residual fracture toughness and residual fiber bridging complementary energy

According to micromechanics [27], the fiber bridging complementary energy J'_b and matrix toughness J_{tip} play an important role in governing ECC tensile ductility, see Fig. 15. Specifically, a lower J_{tip} relative to J'_b promotes flat crack propagation and leading to more cracks. The ratio J'_b/J_{tip} has been suggested by Kanda and Li [27] as an index for quantifying the robustness of tensile ductility in ECC.

The three-point bending test using a notched beam specimen (Fig. 4) was conducted on the ECC matrix (without fiber) according to ASTM E399 [21] to obtain K_m, from which J_{tip} can be calculated ($= K_m^2/E_m$). The modulus of matrix E_m is obtained from the slope of quasi linear segment of load-opening displacement curve. All

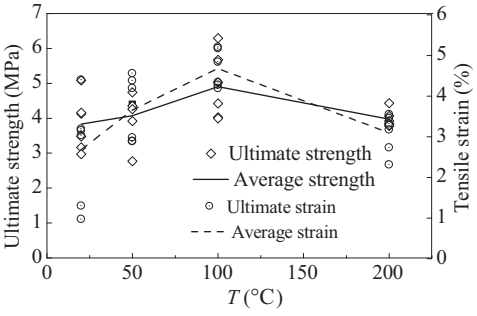

Fig. 8. The effects of temperature exposures on ultimate strength and tensile strain capacity.

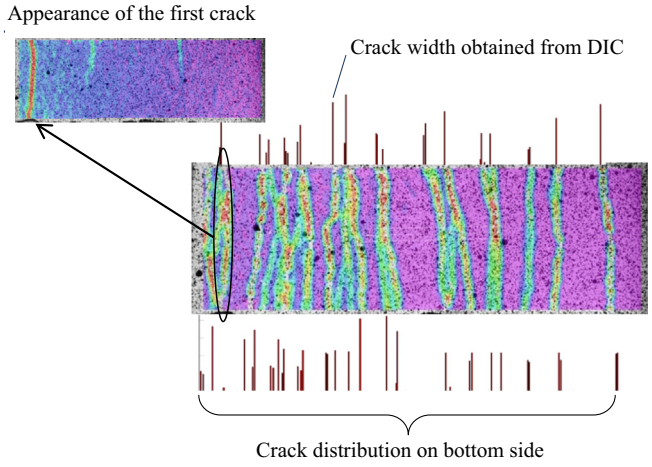

Fig. 9. Typical DIC strain contour of dogbone under tension.

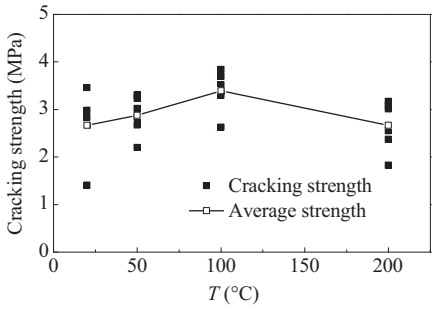

Fig. 10. The effects of temperature exposures on cracking strength.

parametric values in Fig. 16 are normalized by their corresponding values at room temperature.

Single crack tensile test was carried out to calculate J'_b. The resulting fiber-bridging stress and crack open displacement relationship is shown in Fig. 17. Complementary energy J'_b is computed from the area to the left of these curves. Fig. 16 reveals that the residual J'_b is improved for specimens exposed to 50 °C and 100 °C treatments, but experiences a decline after 200 °C exposure.

The J'_b/J_{tip} index and tensile strain capacity of dogbone specimens against temperature are shown in Fig. 18. This trend is consistent with the change in tensile strain capacity as well as the change in the number of micro-cracks of HVFA-ECC exposed to these temperature treatments.

The meso-scale test results provide insights on the mechanisms behind the changes in tensile behavior of HVFA-ECC subjected to temperature exposures. As shown in Fig. 15, the complementary energy J'_b is closely related to the ultimate fiber bridging stress σ_{oc} and the corresponding displacement δ_{oc}. Actually, in meso-scale, J'_b is determined by fiber properties and fiber/matrix interface properties [27]. In the single fiber pull-out test, fiber/matrix interface properties, i.e. the chemical bonding G_d and the frictional bond τ_o, increased after 50 °C and 100 °C exposure, and dropped after 200 °C treatment, making a corresponding variation of the ultimate fiber bridging stress σ_{oc}, provided no premature fiber rupture occurs [27]. As proof, the ultimate strength on dogbone test (Fig. 8) shows the similar trend to those of G_d and τ_o after temperature exposure. Provided J_{tip} and δ_{oc} are the same, enhancing σ_{oc} will lead to more cracks, a higher complementary energy J'_b and eventually a better tensile ductility, just like what occurred in HVFA-ECC after 50 °C and 100 °C treatments.

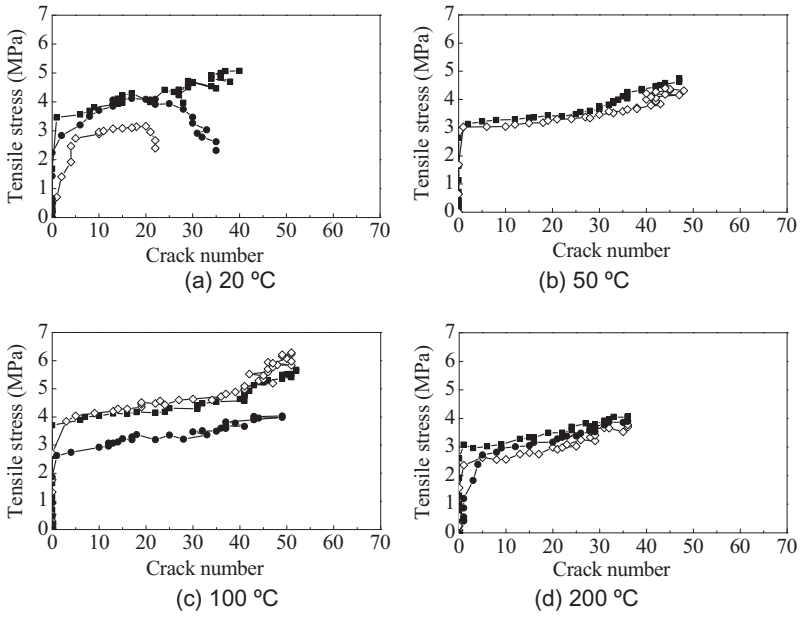

Fig. 11. Crack number development at increasing stress.

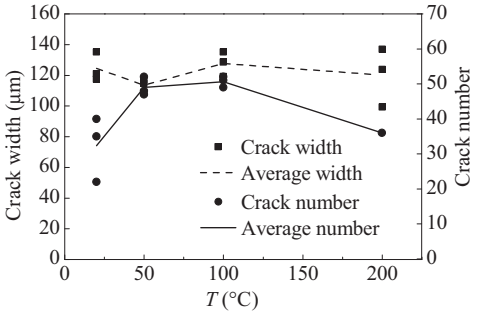

Fig. 12. The effects of temperature exposures on crack width and crack number at peak load.

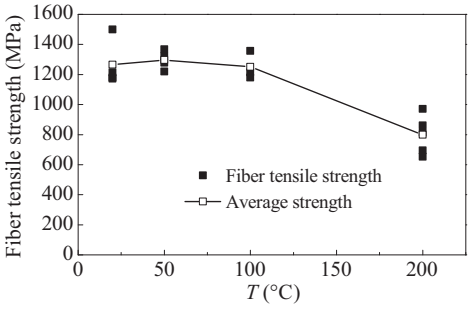

Fig. 13. The effects of temperature exposures on residual fiber strength.

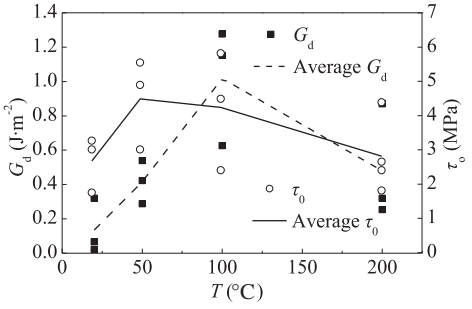

Fig. 14. The effects of temperature exposures on G_d and τ_o.

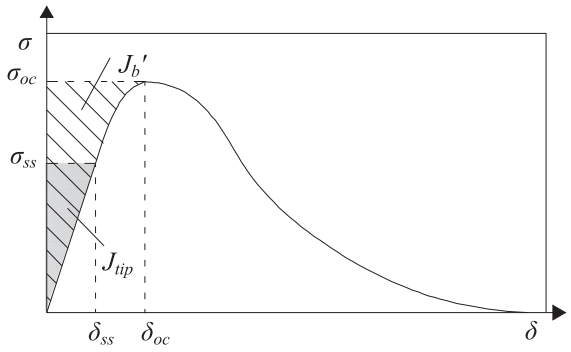

Fig. 15. Typical σ–δ curve for strain-hardening composite. (Hatched area represents complementary energy J_b'. Shaded area represents matrix toughness).

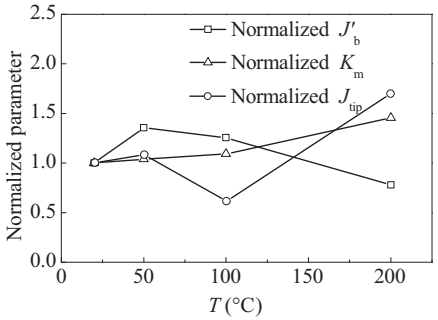

Fig. 16. The effects of temperature exposures on normalized J_b', K_m and J_{tip}.

On the other hand, if σ_{oc} and δ_{oc} keep constant, higher J_{tip} means stronger matrix toughness, and will lead to fewer cracks. Referring to Fig. 16, we can find an obviously higher J_{tip} and a comparatively lower J'_b after 200 °C treatment, leading to a reduction in tensile ductility. The crack number detected by DIC system further confirms this observation.

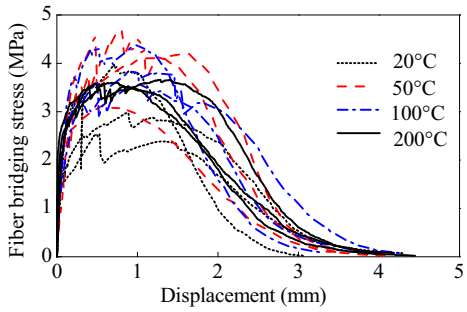

Fig. 17. Fiber-bridging stress vs crack open displacement relationships.

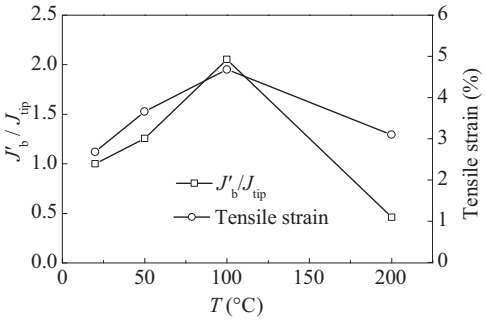

Fig. 18. The effects of temperature exposures on normalized J'_b/J_{tip} and tensile strain capacity.

4. Conclusions

The macro-mechanical properties of ECC with high-volume fly ash after sub-elevated temperature exposures of 50 °C, 100 °C and 200 °C were investigated in this paper. The compressive strength of ECC remained almost unchanged after temperature exposures of 50 °C and 100 °C, but declined after temperature exposure at 200 °C. The axial tensile test indicated HVFA-ECC maintained its unique characteristics of multiple-cracking, strain-hardening and tight crack width control after temperature exposure up to 200 °C for one hour. HVFA-ECC exposed to 50 °C or 100 °C treatment exhibited better residual tensile ductility and strain-hardening behavior than specimens without temperature exposure, but experienced a slight decline after exposure at 200 °C exposures. The DIC measurement indicated that crack widths at ultimate tensile strength remained almost constant at about 120 μm for all specimens with or without temperature exposure. The change of ductility as a result of temperature exposures derives from the change in the number of micro-cracks developed during direct tension tests.

To explain the temperature impact on the mechanical performance of HVFA-ECC, meso-scale tests, including fiber tensile strength test, single fiber pull-out test, three-point bending test and single crack tensile test were carried out to obtain fiber strength, interface parameters (G_d and τ_o), crack tip toughness J_{tip} and complementary energy J'_b as a function of temperature exposures. It was found that a moderate temperature treatment (50 °C or 100 °C) can effectively enhance the fiber/matrix interface properties. The chemical debonding energy G_d and frictional stress τ_o were improved steadily when temperature rose from 20 °C to 100 °C, but decreased slightly at 200 °C. The rise in J'_b/J_{tip} is largely promoted by the improvement in fiber/matrix interface property after exposures of 50 °C and 100 °C, while the drop in J'_b/J_{tip} at 200 °C is largely a result of the loss of this interface property as well as a loss of fiber strength, combined with an increase in J_{tip}. Referring to the pseudo strain hardening criteria, the influence of sub-elevated temperature on HVFA-ECC composite tensile properties is well explained by temperature response at the meso-scale. Additionally, the weakened fiber and fiber/matrix interface after the 200 °C exposure likely make the presence of the fibers act as distributed composite defects that lead to a lower compressive strength.

It should be noted that the above conclusions are drawn based on very high fly ash content ECC with FA/C ratio of 4.4. This high fly ash content may have aided HVFA-ECC in maintaining good residual tensile ductility after the sub-elevated temperature exposures. The knowledge derived provides a sound basis of PVA-ECC design for structural applications in moderately elevated temperature environments. A more systematic study on the influence of fly ash content on residual composite and fiber, matrix and fiber/matrix interface properties is needed to develop a deeper understanding of the role of fly ash on ECC performance after temperature exposure.

Acknowledgments

The authors gratefully acknowledge the financial support of the National Natural Science Foundation of China provided under project: The research of fire resistance of steel members under the protection of light and ultra-toughness cementitious material (51478362). This research was also funded (2013-KF03) by Shanghai Key Laboratory of Engineering Structure Safety (SRIBS), Shanghai, China.

References

[1] B.D. Neeley, D.M. Walley, Very high-strength concrete, The Military Engineer 87 (572) (1995) 36–37.
[2] E.F. O'Neil. On engineering the microstructure of HPCs to improve strength, rheology, and frangibility (PhD dissertation), Northwestern University, Evanston, 2008: 42–8.
[3] V.C. Li, From micromechanics to structural engineering – the 4design of cementitious composites for civil engineering, J. Struct. Mech. Earthquake Eng. 10 (2) (1993) 37–48.
[4] V.C. Li, S. Wang, C. Wu, Tensile strain-hardening behavior of PVA-ECC, ACI Mater. J. 98 (6) (2001) 483–492.
[5] V.C. Li, Engineered cementitious composites – tailored composites through micromechanical modeling, in: N. Banthia, A. Bentur, A. Mufti (Eds.), Fiber Reinforced Concrete: Present and The Future, Canadian Society for Civil Engineering, Montreal, Quebec, Canada, 1998, pp. 64–97.
[6] V.C. Li, C. Wu, S. Wang, A. Ogawa, T. Saito, Interface tailoring for strain-hardening polyvinyl alcohol-engineered cementitious composites (PVA-ECC), ACI Mater. J. 99 (5) (2002) 463–472.
[7] V.C. Li, Tailoring ECC for special attributes: a review, Int. J. Concr. Struct. Mater. 6 (2012) 135–144.
[8] M. Sahmaran, M. Li, V.C. Li, Transport properties of engineered cementitious composites under chloride exposure, ACI Mater. J. 104 (6) (2007) 604–611.
[9] M. Sahmaran, V.C. Li, Durability of mechanically loaded engineered cementitious composites under highly alkaline environment, Cem. Concr. Compos. 30 (2) (2008) 72–81.
[10] M. Sahmaran, V.C. Li, De-icing salt scaling resistance of mechanically loaded engineered cementitious composites, Cem. Concr. Res. 37 (7) (2007) 1035–1046.
[11] S.Z. Qian, V.C. Li, Simplified inverse method for determining the tensile strain capacity of strain hardening cementitious composites, J. Adv. Concr. Technol. 5 (2) (2007) 235–246.
[12] V.C. Li. Strategies for high performance fiber reinforced cementitious composites development [C]. In: Proceedings of International Workshop on Advances in Fiber Reinforced Concrete, Bergamo, Italy, 2000, pp. 93–8.
[13] M. Sahmaran, E. Ozbay, H.E. Yucel, M. Lachemi, V.C. Li, Effect of fly ash and PVA fiber on microstructural damage and residual properties of engineered cementitious composites exposed to high temperatures, J. Mater. Civ. Eng. 23 (12) (2011) 1735–1745.
[14] J.T. Yu, W.F. Weng, K.Q. Yu, Effect of different cooling regimes on the mechanical properties of cementitious composites subjected to high temperatures, Sci. World J. 2014 (2014) 1–7.
[15] M. Sahmaran, M. Lachemi, V.C. Li, Assessing mechanical properties and microstructure of fire-damaged engineered cementitious composites, ACI Mater. J. 107 (3) (2010) 297–304.

[16] P.S. Bhat, V. Chang, M. Li, Effect of elevated temperature on strain-hardening engineered cementitious composites, Constr. Build. Mater. 69 (2014) 370–380.
[17] V. Mechtcherine, F.D. Silva, S. Muller, P. Jun, R.D. Toledo, Coupled strain-rate and temperature effects on the tensile behavior of strain-hardening cement-based composites (SHCC) with PVA fibers, Cem. Concr. Res. 42 (2012) 1417–1427.
[18] JSCE, Recommendations for design and construction of high performance fiber reinforced cement composites with multiple fine cracks, Japan Society of Civil Engineers, Tokyo, 2008. pp. 1–16.
[19] W.H. Peter, W.F. Ranson, Digital imaging techniques in experimental stress analysis, Opt. Eng. 21 (1981) 427–431.
[20] C. Redon, V.C. Li, C. Wu, H. Hoshiro, T. Saito, A. Ogawa, Measuring and modifying interface properties of PVA fibers in ECC matrix, J. Mater. Civ. Eng. 13 (6) (2001) 399–406.
[21] ASTM E399-12, Standard test method for linear-elastic plane-strain fracture toughness KIC of metallic materials, ASTM International, West Conshohocken (PA), 2012.
[22] T. Kanda, V.C. Li, Interface property and apparent strength of a high strength hydrophilic fiber in cement matrix, J. Mater. Civ. Eng. 10 (1) (1998) 5–13.
[23] Z. Lin, T. Kanda, V.C. Li, On interface property characterization and performance of fiber reinforced cementitious composites, J. Concr. Sci. Eng. 1 (1999) 173–184.
[24] V.C. Li, H. Stang, Interface property characterization and strengthening mechanisms in fiber reinforced cement based composites, Adv. Cem. Based Mater. 6 (1) (2002) 1–20.
[25] W.P.S. Dias, G.A. Khoury, P.J.E. Sullivan, Mechanical properties of hardened cement paste exposed to temperatures up to 700 °C (1292F), ACI Mater. J. 87 (2) (1990) 160–166.
[26] G.A. Khoury, Compressive strength of concrete at high temperatures: a reassessment, Mag. Concr. Res. 44 (161) (1992) 291–309.
[27] T. Kanda, V.C. Li, New micromechanics design theory for pseudo strain hardening cementitious composite, ASCE J. Eng. Mech. 125 (4) (1999) 373–381.